University of Massachusetts Boston

ScholarWorks at UMass Boston

Physics Faculty Publications   Physics

Carrier dynamics of terahertz emission based on strained SiGe/Si single quantum well

K. M. Hung
National Kaohsiung University of Applied Sciences

J.-Y. Kuo
National Kaohsiung University of Applied Sciences

C. C. Hong
National Taiwan University

Greg Sun
University of Massachusetts Boston, greg.sun@umb.edu

R. A. Soref
Air Force Research Laboratory, Hanscom Air Force Base

Recommended Citation

Hung, K. M.; Kuo, J.-Y.; Hong, C. C.; Sun, Greg; and Soref, R. A., "Carrier dynamics of terahertz emission based on strained SiGe/Si single quantum well" (2010). *Physics Faculty Publications*. 9.
https://scholarworks.umb.edu/physics_faculty_pubs/9

Carrier dynamics of terahertz emission based on strained SiGe/Si single quantum well

K. M. Hung, J.-Y. Kuo, C. C. Hong, H. H. Cheng, G. Sun et al.

Related Articles

Vertical nonpolar growth templates for light emitting diodes formed with GaN nanosheets
Appl. Phys. Lett. 100, 033119 (2012)

Irregular spectral position of E || c component of polarized photoluminescence from m-plane InGaN/GaN multiple quantum wells grown on LiAlO2
Appl. Phys. Lett. 99, 232114 (2011)

Improvement in spontaneous emission rates for InGaN quantum wells on ternary InGaN substrate for light-emitting diodes
J. Appl. Phys. 110, 113110 (2011)

Influence of high temperature AlN buffer on optical gain in AlGaN/AlGaN multiple quantum well structures
Appl. Phys. Lett. 99, 171912 (2011)

Two-color InGaN/GaN microfacet multiple-quantum well structures grown on Si substrate
J. Appl. Phys. 110, 083518 (2011)

Additional information on Appl. Phys. Lett.

Journal Homepage: http://apl.aip.org/

Journal Information: http://apl.aip.org/about/about_the_journal

Top downloads: http://apl.aip.org/features/most_downloaded

Information for Authors: http://apl.aip.org/authors

Carrier dynamics of terahertz emission based on strained SiGe/Si single quantum well

K. M. Hung,[1] J.-Y. Kuo,[1] C. C. Hong,[2] H. H. Cheng,[2,a)] G. Sun,[3] and R. A. Soref[4]

[1]*Department of Electronics Engineering, National Kaohsiung University of Applied Sciences, Kaohsiung 807, Taiwan*
[2]*Center for Condensed Matter Sciences and Graduate Institute of Electronics Engineering, National Taiwan University, Taipei 106, Taiwan*
[3]*Department of Physics, University of Massachusetts–Boston, Boston, Massachusetts 02125, USA*
[4]*Sensors Directorate, Air Force Research Laboratory, Hanscom AFB, Massachusetts 01731, USA*

We report analysis of the carrier distribution during terahertz emission process with carrier–phonon interaction based on p-doped strained SiGe/Si single quantum-well. The results of this analysis show that a considerable number of carriers can penetrate the phonon wall to become "hot" carriers on an approximately picosecond timescale. These hot carriers relax after the removal of the applied voltage, generating a "second" emission in the measurement. This investigation provides an understanding of the carrier dynamics of terahertz emission and has an implication for the design of semiconductor terahertz emitters. © *2010 American Institute of Physics*. [doi:10.1063/1.3432075]

The development of semiconductor light sources in the energy range of terahertz (THz) has attracted a great deal of attention in recent years.[1–10] In group-IV p-type doped structures, THz emission has been reported in both bulk Ge and strained SiGe single quantum well (SQW) structures.[1–6] In both these cases, the energy band of the valence band is split into heavy-hole (HH) and light-hole (LH) bands. Emission has been attributed to the optical transition of electrically excited carriers between the impurity levels associated with the HH and LH bands. The dynamics of these carriers has been characterized by a streaming motion under the consideration that the energy of the excited carriers can only increase up to that of optical phonons before being scattered, because of the presence of a "hard" phonon wall. A previous theoretical analysis of the carrier distribution under an applied electric field indicated the occurrence of population inversion;[5,6] this led to investigations for obtaining a better understanding of the emission mechanism and for improving the emission efficiency.

We report analysis of the carrier dynamics of the THz emission with carrier–phonon interaction on the p-doped strained SiGe/Si SQW structure. The results show that the electrically excited carriers attain the LO-phonon energy within the timescale of picosecond and a considerable number of carriers move beyond the LO-phonon energy level to become "hot" carriers. These hot carriers relax after the removal of the applied voltage, generating a "second" emission as demonstrated in the measurement.

The sample used in this study was grown by Molecular Beam Epitaxy (MBE) on n-type Si (100) substrate (10^4 Ω cm). It comprises (a) a 100-nm-thick undoped Si buffer layer, (b) a 20-nm-thick $Si_{0.85}Ge_{0.15}$ layer with boron δ-doped at the center, and (c) a 20-nm-thick Si capping layer with boron δ-doped at the center. The doping concentrations for layers (b) and (c) are determined to be 5×10^{11} cm^{-2} by the technique of secondary ion mass spectrometry. The

sample was cut into 1 cm^2 squares with four polished sides. Aluminum contact electrodes, separated by 6 mm, were deposited on top of the sample. This was followed by rapid thermal annealing to allow Al to diffuse into the SiGe middle layer to form Ohmic contacts. The resistivity of the sample is 7.5 kΩ cm at 4.2 K. The SiGe SQW is under in-plane compressive strain and the HH band lie below the LH band. A schematic of the flat valence band profile along the growth direction is plotted in Fig. 1. Quantum confinement results in the formation of confined subband levels. For the HH and LH subbands, the ground state is denoted by E_{HH} and E_{LH}, respectively. The associated ground-state acceptor levels for the two ground states are denoted as E_{HH}^{1S} and E_{LH}^{1S}, respectively. The energy splitting between E_{HH} and E_{LH} is 32 meV, and the LO-phonon energy is $\hbar\omega_{LO}=59.1$ meV[3] for the structure described above.

Under an electrical field applied along the SQW plane, the free carriers located at the bottom of HH subband gain energy following the in-plane dispersion relationship of the HH subband. A schematic diagram of the in-plane dispersion
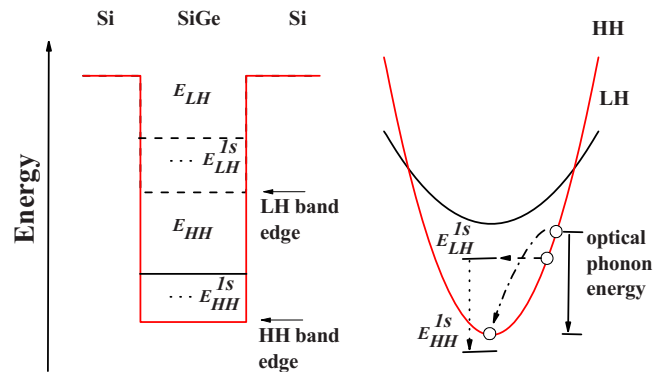

FIG. 1. (Color online) Left: Schematic diagram of SiGe SQW valence band profile along the growth direction. The confined levels of HH and LH bands are denoted as E_{HH} and E_{LH} and their associated acceptor levels are denoted as E_{HH}^{1S} and E_{LH}^{1S}, respectively. Right: in-plane dispersion curve of the two bands. Carrier dynamics showing the three processes of (1) resonant tunneling, (dashed arrow line), (2) THz optical transition (dotted arrow line), and (3) LO-phonon scattering (dashed-dotted arrow line).

a)Author to whom correspondence should be addressed. Electronic mail: hhcheng@ntu.edu.tw.

curve for both the HH and the LH subbands is plotted in Fig. 1. As carriers accelerate toward high energy levels, the following two processes occur: (a) as the carrier energy approaches that of E_{LH}^{1S}, some of the carriers undergo resonant tunneling to occupy the acceptor level E_{LH}^{1S} (indicated by the dashed arrow line) while the rest continue to accelerate toward higher energy levels. Those carriers that have tunneled to the E_{LH}^{1S} state can then fall to the lower-energy acceptor states of E_{HH}^{1S}, yielding THz emission (indicated by the dotted arrow line). The remaining carriers continue to accelerate, passing the energy level E_{LH}^{1S}. (b) Upon reaching the energy level of the LO-phonon, a "hard" phonon wall is imposed where all the carriers are scattered by the emission of optical phonons and relax toward the top of the HH subband (indicated by the dashed-dotted arrow line). These relaxed carriers repeatedly undergo the two processes described above; this process is referred to as "streaming motion."

The time-dependent carrier distribution function ($f_{\vec{k}}$) can be expressed as follows:[5,6]

$$\frac{\partial f_{\vec{k}}}{\partial t} + \frac{eF}{\hbar}\frac{\partial f_{\vec{k}}}{\partial k_x} = \left.\frac{\partial f_{\vec{k}}}{\partial t}\right|_{tunnel} + \left.\frac{\partial f_{\vec{k}}}{\partial t}\right|_{elastic}, \quad (1)$$

where $\vec{k}=k_x\hat{i}+k_y\hat{j}$ is the in-plane carrier-momentum vector and F is the strength of the electric field. The terms on the right-hand side of Eq. (1) represent the rate of change in $f_{\vec{k}}$ associated with the tunneling process (first term) and carrier-impurity elastic scattering (second term). It is observed that population inversion occurs between the energy level of the excited state of E_{LH}^{1S} and several impurity levels of the HH subband; this population inversion is attributed to the slow recombination rate for the E_{LH}^{1S} to E_{HH}^{1S} transition as compared to the timescale of the carriers reaching the energy level of E_{LH}^{1S}.[5,6]

Here, we have "softened" the phonon wall by including the carrier–phonon interaction in the modeling. The rate equation of LO-phonon scattering is given by[11,12]

$$\left.\frac{\partial f_{\vec{k}}}{\partial t}\right|_{LO-phonon} = \sum_{\vec{q}} \frac{|D_{\vec{q}}|^2}{\hbar q^2}\delta(E_{\vec{k}} - E_{\vec{k}+\vec{q}} - \hbar\omega_{LO})(f_{\vec{k}+\vec{q}} - f_{\vec{k}}), \quad (2)$$

where $D_{\vec{q}}$ is the carrier–LO-phonon coupling constant and is defined as $|D_{\vec{q}}|^2=[1/\varepsilon_\infty - 1/\varepsilon_0]e^2\hbar\omega_{LO}/2Ad$, where $\varepsilon_\infty(\varepsilon_0)$ is the dielectric constants at high(zero) frequencies. A is the sample area and d is the thickness of the SQW. Using the parameters from references[5,6] for Eq. (1) and a free carrier concentration of $E_f=1$ meV, $f_{\vec{k}}$ is calculated for a range of electric fields from 100 to 1500 V/cm applied along the x-direction. A color contour profile for an electric field of 1200 V/cm and the spectra recorded at $k_y=0$ are plotted in Fig. 2. At $t=0$ [Fig. 2(a)], $f_{\vec{k}}$ is centered at the zone center of the HH subband with $k_x^2+k_y^2=0$. As t increases, $f_{\vec{k}}$ elongates along the field direction and the peak amplitude of $f_{\vec{k}}$ reduces as the carrier energy increases, as shown in the spectra [Figs. 2(b)–2(d)]. This decrease in the peak amplitude of $f_{\vec{k}}$ is attributed to various scattering processes. At $t=1$ ps [Fig. 2(b)], as the energy of the carriers approaches the acceptor level of E_{LH}^{1S}, which is denoted by the red dashed line, the following two processes occur. First, a few carriers are scattered back to the energy region of the HH zone center, as shown by the weak feature in the spectrum indicated by the solid arrow line; this scattering is attributed to the elastic
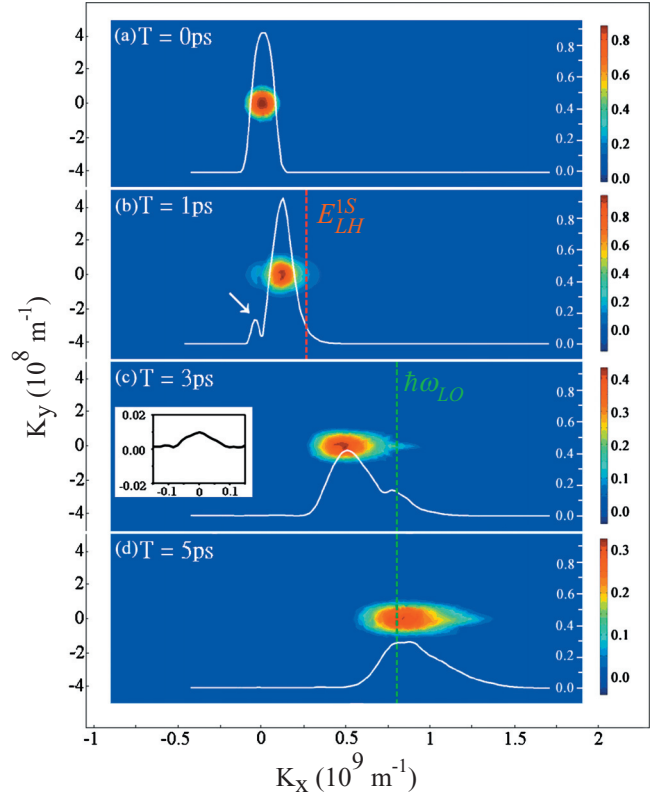

FIG. 2. (Color) Contour diagram of time evolution of carrier distribution function plotted as a function of k_x and k_y. Spectra for $k_y=0$ are also shown. Electric field of 1200 V/cm is applied along the k_x-direction. The colored mark on the left-hand side indicates the intensity of the distribution function.

scattering described above. Second, carriers undergo resonant tunneling to occupy the E_{LH}^{1S} state and subsequently fall to the E_{HH}^{1S} state, leading to THz emission. At around $t=3$ ps [Fig. 2(c)], most of the carriers cross the resonant state of E_{LH}^{1S} and acquire energies that are approximately equal to the LO-phonon energy (denoted by the green dashed line). The distribution function broadens because of LO-phonon scattering. At this point, the energy levels of some carriers become higher than the LO-phonon energy level, while very few carriers appear in the energy region of the HH zone center, as indicated by the weak amplitude in the spectrum plotted in the inset; this is attributed to the low coupling strength of the carrier–LO-phonon interaction. At $t=5$ ps [Fig. 2(d)], $f_{\vec{k}}$ broadens further as more carriers are subjected to phonon scattering. However, a considerable number of carriers are distributed beyond the LO-phonon energy level. A similar behavior is also observed under other electric fields. Under low electric fields, carriers penetrate the phonon wall with a longer time; the opposite behavior is observed for large voltages.

The measurement of the THz emission from our sample was conducted as follows. A voltage pulse generator was used for electrical excitation; this generator produces a square pulse voltage with a pulse magnitude up to 1000 V and a pulse duration of $1-14$ μs (AVTEC). A resistor with a resistance of 1 Ω was placed in series with the sample in order to measure the current. For THz detection, a Ga-doped Ge detector was used. The detector was first calibrated by both electrical and optical measurements at a temperature of ~ 6 K. Electrical measurement revealed that the detector exhibited an electrical characteristic similar to that of a conven-
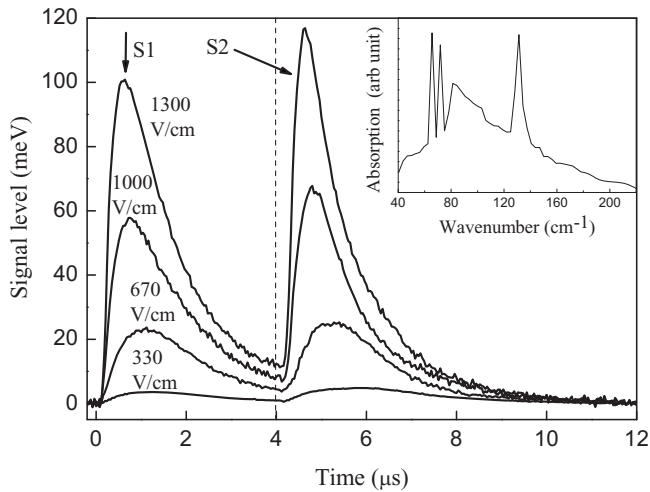
FIG. 3. Measured signal level at different applied voltages with a pulsed duration of 4 μs. Dashed line marks the removal of applied pulsed voltage. Inset: absorption spectrum of the photodetector.

tional PN junction, wherein at an applied voltage of $\sim$2 V, the current increases rapidly. Optical characterization was performed using Fourier transform infrared spectroscopy equipped with a helium-cooled Si bolometer. The spectrum showed that the detector responded to an energy range from $\sim$50 to 150 cm^{-1} with two sharp transitions with peak positions at 68 and 74 cm^{-1} and a reasonably sharp transition with a peak position at 137 cm^{-1} (The absorption spectrum of the detector is shown as insert of Fig. 3). THz emission within this range will induce a photocurrent in the detector which was biased at the onset of 2 V. Measurements of the emission from the sample were performed at a low temperature of 4.2 K, with both the sample and the detector immersed in liquid helium. The detector was placed near the sample at a distance of about 5 mm.

A family of recorded signals with different pulsed voltages of a duration of 4 μs is shown in Fig. 3. Two distinct signals are clearly resolved; one (labeled S1) appeared within the pulse duration ($t < 4$ μs) and another (labeled S2) after the applied pulsed voltage was switched off. Signal S1 is associated with the optical transition of $E_{LH}^{1S} \rightarrow E_{HH}^{1S}$ as discussed above. For signal S2, the emission is associated with those carriers that exhibit energies greater than the phonon

energy. These hot carriers relax after the removal of the applied voltage. As the carriers pass through the energy level in resonance with the E_{LH}^{1S} state, they can once again tunnel to the E_{LH}^{1S} state and undergo a transition to the E_{HH}^{1S} state, yielding a second THz emission.

In summary, we have presented the analysis of the carrier dynamics of THz emission by taking into account the carrier–phonon interaction. The results show that most of the carriers cross the LO-phonon energy level. This suggests that the mechanism of streaming motion employed previously is not supported. These findings provide a practical understanding of the carrier dynamic during THz emission process and can assist the design of semiconductor THz emitters.

[1] I. V. Altukhov, E. G. Chirkova, M. S. Kagan, K. A. Korolev, V. P. Sinis, M. A. Odnoblyudov, and I. N. Yassievich, Sov. Phys. JETP **88**, 51 (1999).
[2] Yu. P. Gousev, I. V. Altukhov, K. A. Korolev, V. P. Sinis, M. S. Kagan, E. E. Haller, M. A. Odnoblyudov, I. N. Yassievich, and K. A. Chao, Appl. Phys. Lett. **75**, 757 (1999).
[3] A. Blom, M. A. Odnoblyudov, H. H. Cheng, and K. A. Chao, Appl. Phys. Lett. **79**, 713 (2001).
[4] I. V. Altukhov, E. G. Chirkova, V. P. Sinis, M. S. Kagan, Yu. P. Gousev, S. G. Thomas, K. L. Wang, M. A. Odnoblyudov, and I. N. Yassievich, Appl. Phys. Lett. **79**, 3909 (2001).
[5] M. A. Odnoblyudov, I. N. Yassievich, M. S. kagan, Y. M. Galperin, and K. A. Chao, Phys. Rev. Lett. **83**, 644 (1999).
[6] M. A. Odnoblyudov, I. N. Yassievich, V. M. Chistyakov, and K. A. Chao, Phys. Rev. B **62**, 2486 (2000).
[7] A. Borak, S. Tsujino, C. Falub, M. Scheinert, L. Diehl, E. Müller, H. Sigg, D. Grützmacher, U. Gennser, I. Sagnes, S. Blunier, T. Fromherz, Y. Campidelli, O. Kermarrec, D. Bensahel, and J. Faist, Mater. Res. Soc. Symp. Proc. **832**, p. F4.2.1 (2005).
[8] S. Tsujino, H. Sigg, M. Scheinert, D. Grützmacher, and J. Faist, IEEE J. Sel. Top. Quantum Electron. **12**, 1642 (2006).
[9] S. A. Lynch, P. Townsend, G. Matmon, D. J. Paul, M. Bain, H. S. Gamble, J. Zhang, Z. Ikonic, R. W. Kelsall, and P. Harrison, Appl. Phys. Lett. **87**, 101114 (2005).
[10] S. G. Pavlov, H.-W. Hübers, J. N. Hovenier, T. O. Klaassen, D. A. Carder, P. J. Phillips, B. Redlich, H. Riemann, R. K. Zhukavin, and V. N. Shastin, Phys. Rev. Lett. **96**, 037404 (2006).
[11] K. Hess, *Advanced Theory of Semiconductor Devices* (Prentice-Hall, New Jersey, 1988).
[12] P. Lawaetz, Phys. Rev. B **4**, 3460 (1971).